[CANCER RESEARCH 62, 156–164, January 1, 2002]

Mechanisms of Cell Cycle Arrest by Methylseleninic Acid[1]

Zongjian Zhu, Weiqin Jiang, Howard E. Ganther, and Henry J. Thompson[2]

Center for Nutrition in the Prevention of Disease, AMC Cancer Research Center, Lakewood, Colorado 80214 [Z. Z., W. J., H. J. T.], and Department of Nutritional Sciences, University of Wisconsin, Madison, Wisconsin 53706 [H. E. G.]

ABSTRACT

Methylseleninic acid (MSA) is a monomethylated form of selenium effective in inhibiting cell growth *in vitro* and experimental mammary carcinogenesis *in vivo*. MSA offers particular advantage in cell culture experiments because it is stable in solution and provides a monomethylated form of selenium that can be reduced by cellular reducing systems and released nonenzymatically within a cell. In the present study, MSA was used to elucidate the mechanisms of cell growth inhibition by selenium. These studies were performed using a mouse mammary hyperplastic epithelial cell line, TM6. MSA induced a rapid arrest of synchronized cells in the G_1 phase of the cell cycle. This effect was accompanied by a reduction in total cellular levels of cyclin D1. Whereas MSA had no effect on total levels of the cyclin-dependent kinase (CDK)4, the amount of CDK4 immunoprecipitated with cyclin D1 in MSA-treated cells was decreased as was the kinase activity of the immunoprecipitated complex. MSA did not significantly affect cyclin E or associated regulatory molecules. Treatment with MSA suppressed the hyperphosphorylated form of retinoblastoma (Rb) with a commensurate increase in the hypophosphorylated form. Levels of E2F-1 bound to Rb also were elevated. Levels of insulin-like growth factor-I receptor and phosphorylated Akt were reduced by MSA. It is concluded that MSA induces a G_1 arrest in the cell cycle. This effect may be induced by MSA via its modulation of insulin-like growth factor-I-mediated signal transduction leading to inhibition of Akt activation and limitation of cyclin D1-CDK4-mediated phosphorylation of Rb.

INTRODUCTION

Selenium is a potent chemopreventive agent in animal model systems, and accumulating evidence indicates that selenium also protects against the development of cancer in human populations (1–5). However, a significant limitation in the translation of existing laboratory data to the clinic is the lack of information about the form of selenium that is likely to be most efficacious for cancer prevention. This is a particularly important point because laboratory experiments indicate that the chemical form in which selenium is ingested can have a profound effect on its biological activity, including its ability to inhibit the development of cancer (6–8). One approach that is likely to help resolve the issue of the form of selenium to use clinically is the identification of both the specific chemical species of selenium that inhibits the development of cancer and the target molecule(s) through which selenium mediates its chemopreventive activity. Currently, available evidence points to a monomethylated form of selenium as being either a direct precursor or the active species of selenium for cancer prevention (1, 7). However, identification of the target molecule(s) on which the active selenium species exerts its effect has been more elusive. What has been determined to date is that monomethylated forms of selenium that inhibit mammary carcinogenesis in animal model systems have two prominent activities on cells in culture: the inhibition of their proliferation and the induction of their death via apoptosis (7). Because other published work indicates that various selenium compounds may regulate specific steps in the cell cycle (9–13), and because defects in cell cycle control are commonly observed in human cancers (14, 15), experiments were performed using a recently developed monomethylated selenium compound, MSA[3] (1), which rapidly releases within the cell a form of selenium hypothesized to be involved in cancer prevention. The experiments were conducted using a mouse mammary hyperplastic epithelial cell line, TM6, because selenium has been reported to be most effective in preventing the progression of mammary hyperplasias to carcinoma (7, 9–13, 16, 17). The goal of the experiments reported in this study was to identify the specific phase(s) of the cell cycle and the components of the cell cycle machinery that are regulated by MSA using a combination of pathway-specific cDNA array-guided assays coupled with detailed analyses of changes in amounts and/or activities of cell cycle regulatory molecules.

MATERIALS AND METHODS

Chemicals. The following materials were purchased from commercial sources: DMEM and F-12 medium (Sigma Chemical Co., St. Louis, MO); adult bovine serum (Gemini Bioproducts, Calabasas, CA); insulin and EGF (Intergen, Purchase, NY); gentamicin reagent solution (Life Technologies, Inc., Grand Island, NY); BrdUrd cell proliferation assay kit (Oncogene, Cambridge, MA); anticyclin D1, anti-CDK4, anti-CDK2, anti-P21, anti-P27, anti-P16, anti-P19, and anti-E2F-1 antibodies (Neomarkers, Inc., Fremont, CA); Rb-GST fusion protein, protein A/G PLUS-agarose, and anticyclin E and anti-IGF-IR antibodies, rabbit antimouse immunoglobulin- and goat antirabbit immunoglobulin-horseradish peroxidase-conjugated secondary antibodies (Santa Cruz Biotechnology Corp., Santa Cruz, CA); histone H1 (Boehringer Mannheim Corp., Indianapolis, IN); anti-Rb antibody (PharMingen/Transduction Laboratories, San Diego, CA); anti-ppAkt and antitotal Akt antibodies (Cell Signaling Technology, Beverly, MA); [γ-^{32}P]ATP (specific activity 3000 Ci/mmol; Amersham Pharmacia Biotech, Piscataway, NJ); and ECL detection system (Amersham Life Science, Inc., Arlington Heights, IL). The MSA was synthesized by H. E. Ganther (7).

Standard Cell Culture Conditions. The mouse mammary hyperplastic epithelial cell line TM6 was obtained from the laboratory of Daniel Medina (18, 19). Cells were maintained at 37°C in a humidified incubator containing 5% CO_2. The cells were grown in DMEM and F-12 medium (1:1 DMEM:F-12) containing 2% adult bovine serum, 10 μg/ml insulin, 5 ng/ml EGF, and 5 μg/ml gentamicin.

Selenium Treatment. A stock solution of potassium methylseleninate (30 mM) was diluted 100-fold with PBS (pH 7.4) immediately before use. The pH of the working solution remained at 7.4. The working solution was added to cell culture media to achieve the desired selenium concentration. The cells were then exposed to the MSA supplemented media.

Synchronization of TM6 Cells. TM6 cells were synchronized as described previously (12). Briefly, cells were allowed to grow for 48 h in regular medium (containing insulin, EGF, and serum), after which, the cells were starved by deprivation of growth factors and serum for another 48 h. Cells were released from growth arrest by feeding them regular medium (containing growth factors and serum) for 6 h, at which time, cells were treated with MSA-supplemented media as described above.

Received 7/5/01; accepted 10/30/01.

The costs of publication of this article were defrayed in part by the payment of page charges. This article must therefore be hereby marked *advertisement* in accordance with 18 U.S.C. Section 1734 solely to indicate this fact.

[1] Supported by Grant No. CA45164 from the National Cancer Institute.

[2] To whom requests for reprints should be addressed, at AMC Cancer Research Center, 1600 Pierce Street, Denver, CO 80214. Phone: (303) 239-3463; Fax: (303) 239-3443; E-mail: thompsonh@amc.org.

[3] The abbreviations used are: MSA, methylseleninic acid; ECL, enhanced chemiluminescence; CDK, cyclin dependent kinase; Rb, retinoblastoma; IGF-IR, insulin like growth factor I receptor; ppAkt, phosphorylated Akt; EGF, epidermal growth factor; GST, glutathione *S*-transferase; GAPDH, glyceraldehyde-3-phosphate dehydrogenase; CKI, cyclin dependent kinase inhibitor; INK, inhibitor of cyclin dependent kinase.

Cell Proliferation Analysis By BrdUrd Labeling. Cell proliferation was determined using a BrdUrd Cell Proliferation Assay Kit (Oncogene). Briefly, TM6 cells cultured in 96-well plates were synchronized and released as described above and were exposed to either 0 or 5 μM MSA for 0.5, 1, 2, or 3 h. After exposure to MSA, cells were rinsed once with sterile solution A [10 mM glucose, 130 mM NaCl, 3 mM KCl, 1 mM Na_2HPO_4, 30 mM HEPES, and 3.3 μM phenol red (pH 7.6)] and then were given fresh media (without MSA) to which BrdUrd was added. Cells were pulse labeled for an additional 2 h with BrdUrd and then fixed. Incorporation of BrdUrd was detected by immunoreaction using mouse anti-BrdUrd antibody and goat antimouse IgG horseradish peroxidase conjugate. After substrate solution was added to each well, the amount of BrdUrd incorporated was determined by measuring absorbance at dual wavelengths 450–540 nm using a spectrophotometric $Thermo_{max}$ Microplate Reader (Molecular Devices, Sunnyvale, CA).

Analyses of Cell Cycle Distribution. After treatment of synchronously growing TM6 cells with 0 or 5 μM MSA for 0.5, 1, 2, or 3 h, cells were enzymatically dissociated. The nuclei were stained with propidium iodide using a procedure described by Krishan (20) and subjected to fluorescence-activated cell sorter analysis performed at the University of Colorado Health Sciences Center Flow Cytometry Core Facility.

Expression of Cell Cycle Regulatory Molecules By Immunoprecipitation and Western Blotting. TM6 cells were cultured using the synchronous model as described above in assessing the expression of cyclin D1 and CDK4, the binding of CDK4 to cyclin D1, cyclin D1-associated kinase activity (Rb-GST), P19, cyclin E, CDK2, the binding of CDK2 to cyclin E, cyclin E-associated kinase activity (histone H1), P21, the binding of P21 to cyclin E, P27, the binding of P27 to cyclin E, product of Rb, E2F-1, binding of E2F-1 to Rb, IGF-IR, ppAkt, and total Akt. Synchronized TM6 cultures were treated with 0 or 5 μM MSA for 0.5, 1, 2, or 3 h after 48-h starvation and 6-h refeeding.

For all experiments, the media were aspirated at the end of the specified treatment period, and the monolayer of cells was quickly washed two times with cold PBS. A 0.3-ml aliquot of lysis buffer [10 mM Tris-HCl (pH 7.4), 150 mM NaCl, 1% Triton X-100, 1 mM EDTA, 1 mM EGTA, 0.2 mM sodium vanadate, 0.2 mM phenylmethylsulfonyl fluoride, 0.5% NP-40, and 0.2 units/ml aprotinin] was then added per plate. After bathing in lysis buffer for 15 min on ice, the cells were scraped from the plate, and the mixture of buffer and cells was transferred to microfuge tubes and left in ice for an additional 15 min. The lysate was collected by centrifugation for 15 min in an Eppendorf centrifuge at 4°C, and protein concentration in the clear supernatant was determined by the Bio-Rad protein assay (Bio-Rad, Hercules, CA). For Western blotting of cell cycle regulatory molecules, 40 μg of protein lysate/sample were denatured with SDS-PAGE sample buffer [63 mM Tris-HCl (pH 6.8), 10% glycerol, 2% SDS, 0.0025% bromphenol blue, and 5% 2-mercaptoethanol] and subjected to SDS-PAGE on an 8% or 12% gel, and the protein bands were blotted onto a nitrocellulose membrane (Invitrogen, Carlsbad, CA). The levels of cyclin D1, CDK4, P16, P19, cyclin E, CDK2, P21, P27, Rb, E2F-1, IGF-IR, ppAkt, and total Akt were determined using the specific primary antibodies designated above, followed by treatment with the appropriate peroxidase-conjugated secondary antibody and visualized by the ECL detection system. For studies evaluating CDK4 binding to cyclin D1, CDK2, and P21 or P27 binding to cyclin E and E2F-1 binding to Rb, 200 μg of protein lysate/sample were mixed with 2 μg of anticyclin D1, anticyclin E, or anti-Rb antibody, respectively, and 25 μl of protein A/G PLUS-agrose beads and incubated overnight at 4°C on a rocker platform. On the next day, beads were collected by centrifugation and washed three times with lysis buffer. The immunoprecipitated cyclin D1, cyclin E, or Rb was denatured with the SDS-PAGE sample buffer (composition given above) and subjected to 12 or 8% SDS-PAGE gel followed by Western blotting using a nitrocellulose membrane. The level of CDK4 binding to cyclin D1; of CDK2, P21, or P27 binding to cyclin E; and of E2F-1 binding to Rb was determined by specific primary antibody to CDK4, CDK2, P21, P27, or E2F-1 followed by peroxidase-conjugated antimouse secondary antibody and visualization by the ECL detection system. Signals were quantitated by scanning the film with ScanJet (Hewlett Packard, Palo Alto, CA), and the intensity of the bands was analyzed by using the "Image-Pro Plus" software (Media Cybernetics, Silver Spring, MD).

Kinase Assay. Cyclin D1-associated Rb kinase activity was determined as described previously (21) with some modifications. Briefly, untreated or MSA-treated TM6 cells were lysed in Rb lysis buffer [50 mM HEPES-KOH (pH 7.5), containing 150 mM NaCl, 1 mM EDTA, 2.5 mM EGTA, 1 mM DTT, 0.1% Tween 20, 10% glycerol, 80 mM β-glycerophosphate, 1 mM sodium fluoride, 0.1 mM sodium orthovanadate, 1 mM pheylmethylsulfonyl fluoride, and 10 μg/ml leupeptin and aprotinin], and using anticyclin D1 antibody (2 μg) and protein A/G PLUS-agarose beads (20 μl), specific proteins were immunoprecipitated from 200 μg of protein lysate/sample as described above. Beads were washed three times with Rb lysis buffer and then once with Rb kinase assay buffer [50 mM HEPES-KOH (pH 7.5), containing 2.5 mM EGTA, 10 mM β-glycerophosphate, 1 mM sodium fluoride, 0.1 mM sodium orthovanadate, 10 mM $MgCl_2$, and 1 mM DTT]. Phosphorylation of Rb was measured by incubating the beads with 40 μl of radiolabeled Rb kinase solution [0.25 μl (2 μg) of Rb-GST fusion protein, 0.5 μl of [γ-^{32}P]ATP, 0.5 μl of 0.1 mM ATP, and 38.75 μl of Rb kinase buffer] for 30 min at 37°C. The reaction was stopped by boiling the samples in SDS sample buffer for 5 min. The samples were analyzed by 12% SDS-PAGE, and the gel was dried and subjected to autoradiography. Similarly, cyclin E-associated histone H1 kinase activity was determined as described previously (21) with some modifications. Briefly, using anticyclin E antibody (2 μg) and protein A/G PLUS-agarose beads (20 μl), cyclin E was immunoprecipitated from 200 μg of protein in lysate/sample as detailed above. Beads were washed three times with lysis buffer and then once with kinase assay buffer [50 mM Tris-HCl (pH 7.4), 10 mM $MgCl_2$, and 1 mM DTT]. Phosphorylation of histone H1 was measured by incubating the beads with 40 μl of radiolabeled kinase solution [0.25 μl (2.5 μg) of histone H1, 0.5 μl of [γ-^{32}P]ATP, 0.5 μl of 0.1 mM ATP, and 38.75 μl of kinase buffer] for 30 min at 37°C. The reaction was stopped by boiling the samples in SDS sample buffer for 5 min. The samples were analyzed by 12% SDS-PAGE, and the gel was dried and subjected to autoradiography. Signals were quantitated by scanning the film with ScanJet (Hewlett Packard), and the intensity of the bands was analyzed by using the "Image-Pro Plus" software (Media Cybernetics).

RNA Isolation. Total RNA was isolated from TM6 cells using RNeasy Mini Kit (Qiagen, Valencia, CA) according to the manufacturer's directions. Briefly, after aspirating medium completely, a RLT buffer was added to monolayer cells, and cell lysate was collected with a rubber policeman. The lysate was transferred onto a Qiagen-shredder column sitting in the 2-ml collection tube and centrifuged for 2 min at 15,850 $\times$ *g*. The same volume as the collected lysate of 70% ethanol was added to the homogenized lysate and mixed. The mixture was transferred to an RNeasy mini spin column sitting in a 2-ml collection tube and centrifuged for 15 s at 15,850 $\times$ *g*. After the RNeasy mini column was washed with buffers RW1 and RPE provided by Qiagen, RNA was washed out from the RNeasy column with RNase-free water and collected in a 1.5-ml collection tube. The quality of total RNA was determined by measuring the absorbance at 260 nm (A_{260}) and 280 nm (A_{280}) in a spectrophotometer. The A_{260}/A_{260} ration of samples was 1.9–2.1.

Synthesis of cDNA Probes. Total RNA was used as a template for biotinylated probe synthesis using Nonrad-GEArray Kit (SuperArray, Inc., Bethesda, MD). A 5–10 μg of total RNA was annealed with GEAprimer Mix at 70°C for 2 min and cooled to 42°C. Then, the RNA was labeled with labeling cocktail (Nonrad-GEAlabeling Buffer, biotin-16-dUTP, RNase inhibitor and reverse transcriptase) at 42°C for 120 min. The reaction was stopped, denatured, and neutralized by specific solutions offered by SuperArray, Inc. The resulting cDNA probe was ready to be used for hybridization.

Hybridization and Chemiluminescent Detection. GEArray membrane (SuperArray, Inc.) was prehybridized with GEAhyb Hybridization Solution (SuperArray, Inc.) containing denatured sheared salmon sperm DNA (100 μg of DNA/ml; Life Technologies, Inc.) at 68°C for 2 h and hybridized in the Hybridization Solution (SuperArray, Inc.) containing denatured cDNA probe of the samples at 68°C overnight. After washing the membrane twice with wash solution 1 (300 mM sodium chloride, 30 mM sodium citrate, and 1% SDS) and twice with wash solution 2 (15 mM sodium chloride, 1.5 mM sodium citrate, and 0.5% SDS) for 20 min each at 68°C, the membrane was blocked in GEAblocking solution (SuperArray, Inc.) and incubated in the same solution containing alkaline phosphatase-conjugated streptavidin (1:5000 dilution) for 40 min each at room temperature. After the membrane was washed in a washing buffer (SuperArray, Inc.) three times and rinsed in a rinsing solution (SuperArray, Inc.), the membrane was incubated with chemiluminescent substrate and exposed to X-ray film. Signals were quantitated by scanning the film with ScanJet (Hewlett Packard), and the intensity of the spots was analyzed by using the "Image-Pro Plus" software (Media Cybernetics). β-actin and

Table 1 *Effect of MSA on the proliferation of synchronously growing TM6 cells*

TM6 cells were synchronized by deprivation of growth factors and serum for 48 h and released from synchronization by feeding them regular medium containing growth factors and serum for 6 h. After 6 h refeeding, cells were exposed to either 0 or 5 μM MSA for 0.5, 1, 2, or 3 h. All experiments were repeated three times. In each experiment, eight replicates at each time point were analyzed. The results of a representative experiment are presented. Data are expressed as mean ± SE and were analyzed by ANOVA with posthoc comparisons by the method of Bonferroni. Values within a column with different superscripts are statistically different from each other, $P < 0.001$.

Exposure (h)	Control (MSA, 0 μM) Absorbance	MSA, 5 μM Absorbance
0.5	0.078 ± 0.005^{a}	0.043 ± 0.005^{a}
1.0	0.112 ± 0.006^{b}	$0.037 \pm 0.004^{a,b}$
2.0	0.210 ± 0.007^{c}	$0.031 \pm 0.004^{a,b}$
3.0	0.273 ± 0.009^{d}	0.025 ± 0.002^{b}

GAPDH were used as a positive control, and bacterial plasmid (pUC18) was used as a negative control.

Statistical Analyses. Differences in the cell proliferation rates of TM6 exposed to MSA at different doses and time points were evaluated by ANOVA (22). Posthoc comparisons among treatment conditions were made using the Bonferroni multiple-range test (22). Data derived from cDNA array or Western blot analyses represent semiquantitative estimates of the amount of a specific mRNA or protein that is present in a cell extract. This fact was taken into account in the statistical evaluation of the data. The data displayed in the graphs are reported as means ± SE of the actual scanning units derived from the densitometric analysis of each cDNA array or Western blot. All values are the means of three different experiments. However, for statistical analyses, the units of scanning density derived from the analysis of the cDNA array or Western blots using Image Pro Plus were first ranked. This approach is particularly suitable for semiquantitative measurements that are collected as continuously distributed data. This approach has the advantage of maintaining the relative relationships among data being compared without giving undue weight to outlying results. The ranked data were then subjected to multivariate ANOVA (22). Statistically, this is a robust approach that takes into account both the fact that levels and/or activities of proteins in a molecular pathway may not vary independently of one another, as well as the issues that exist when multiple comparisons are being made on a particular set of data. Thus, in the multivariate analysis, the question was asked as to whether treatment with MSA, duration of treatment with MSA (time), and/or the interaction between MSA treatment and time (MSA × time) were statistically significant. Only when the overall multivariate statistic for the effect of one of these factors (MSA, time, or MSA × time) on a particular molecular cascade of events was significant were the results of the univariate ANOVAs (which are a component of the multivariate analysis) further considered to ascertain the variables on which MSA, time, or MSA × time were likely to be exerting their effects.

RESULTS

Effects of MSA on Cell Proliferation and Cell Cycle Distribution

The effect of MSA on cell proliferation and cell cycle distribution was evaluated in synchronously growing TM6 cells using the approach described in the "Materials and Methods" section. The dose of selenium was 0 or 5 μM as MSA for 0.5–3 h after 48-h starvation and 6-h refeeding. The proliferation of untreated TM6 cells increased 2.5-fold between 0.5 and 3 h after refeeding, whereas BrdUrd incorporation by TM6 cells treated with 5 μM MSA decreased 42% during the same period ($P < 0.001$; Table 1). When a comparison was made between untreated and MSA-treated TM6 cells at each time point, 5 μM MSA significantly suppressed cell proliferation as early as 0.5 h. The magnitude of reduction in cell proliferation was 45, 67, 85, and 91% in MSA-treated TM6 cells compared with untreated TM6 cells at 0.5, 1, 2, and 3 h of the exposure ($P < 0.001$), respectively (Table 1).

To identify whether cell cycle progression was affected by MSA, the distribution of cells in different phases of cell cycle was determined by flow cytometry. As shown in Fig. 1, the starvation of TM6 cells for 48 h successfully arrested the cells in the G_1 phase of the cell cycle (87%). When the TM6 cells were exposed to 5 μM MSA after 48-h starvation and 6-h refeeding, the proportion of cells in the G_1 phase of the cell cycle increased in comparison to untreated control TM6 cells. The G_1 arrest induced by MSA was observed as early as 0.5 h of exposure. The percentage of MSA-treated cells in G_1 reached a maximum of 95% at 3 h of exposure, whereas only 56% of untreated cells were in G_1 at this time point. In parallel, the proportion of MSA-treated cells in S phase was decreased at each time point relative to the percentage of untreated cells observed in S phase. At 3 h of treatment, the percentage of MSA-treated cells in S phase was 3.2 *versus* 43% for the untreated TM6 cells.

Effects of MSA on Cell Cycle Regulatory Molecules

Gene Array Data. As an initial approach to focusing efforts to investigate the effects of MSA on cell cycle regulatory molecules, total RNA was harvested from synchronized TM6 cells either untreated or treated with 5 μM MSA for 3 h. A commercially available filter array designed for exploring changes in the expression of cell cycle regulatory molecules was used, and the results of a representative experiment are shown in Fig. 2*A*; the coding grid for the filter is also shown. Results from three independent experiments were combined into one data set, and the means and SE were computed and are plotted in Fig. 2*B*. Because multiple endpoints were measured, the probability is increased that differences in gene expression will be found that are attributable to chance alone. To decrease this possibility, the gene expression data were divided into subgroups of genes that are known to be highly related biologically, and the data from each subgroup of genes were subjected to multivariate ANOVA. Specifically, the following statistical questions were posed: are there significant effects attributable to treatment with MSA on the expression of: (*a*) cyclins; (*b*) CDKs; (*c*) members of the INK or Cip/Kip family of CKIs; or (*d*) Rb and E2F. As shown in the tabular portion of Fig. 2*B*, there was a statistically significant effect of MSA on cyclins, CDKs, CKIs, and Rb/E2F. When the strength of the multivariate analysis was considered along with the results of the univariate ANOVA generated

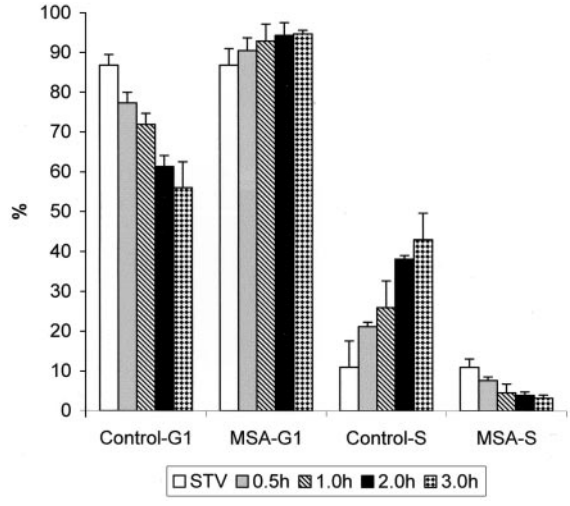

Fig. 1. Time-dependent effects of 5 μM MSA on cell cycle distribution in synchronously growing TM6 cells. After the cells were starved (*STV*) for 48 h and released by feeding with regular medium containing growth factors and serum for 6 h as described in "Materials and Methods," they either remained untreated (*Control*) or were treated with 5 μM MSA for 0.5, 1, 2, and 3 h. Data represent the percentage of cells in G_1 and S phases of the cell cycle. Data are means based on determinations from three independent experiments; *bars*, SE. Only the attached cell population was used for these studies, *i.e.*, floating cells were discarded.

A

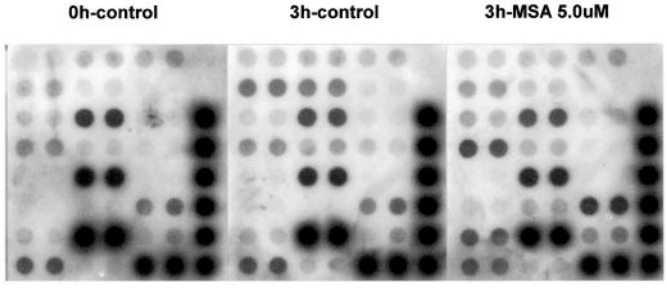

Cdk 2L	Cdk2 L	Cdk 4	Cdk 4	Cdk 6	Cdk 6	pUC18
Cdc2	Cdc2	Cyclin A2	Cyclin A2	Cyclin B	Cyclin B	pUC18
Cyclin C	Cyclin C	Cyclin D1	Cyclin D1	Cyclin D2	Cyclin D2	β-actin
Cyclin D3	Cyclin D3	Cyclin E	Cyclin E	Cyclin E2	Cyclin E2	β-actin
E2F1	E2F1	$p15^{Ink4b}$	$p15^{Ink4b}$	$p16^{Ink4a}$	$p16^{Ink4a}$	GAPDH
p18	p18	p19	p19	$p21^{Cip}$	$p21^{Cip}$	GAPDH
$p27^{Kip1}$	$p27^{Kip1}$	$p57^{Kip2}$	$p57^{Kip2}$	Rb	Rb	GAPDH
skp1	skp1	skp2	skp2	GAPDH	GAPDH	GAPDH

B

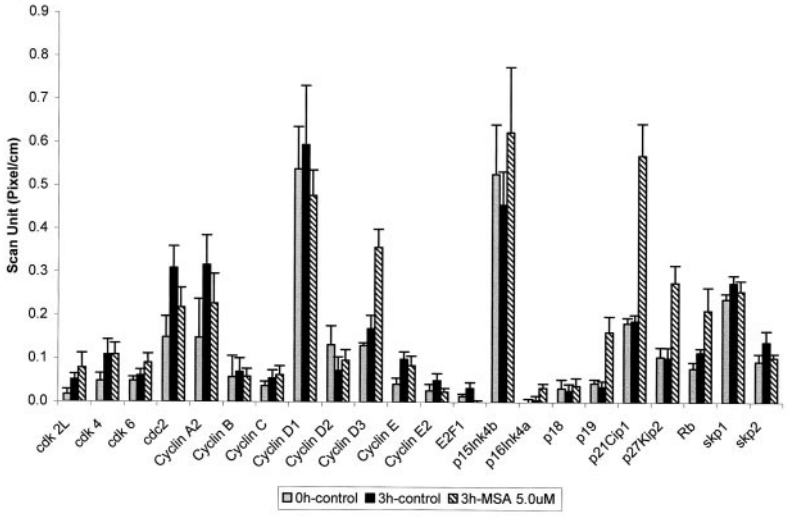

Fig. 2. Cell cycle-specific cDNA array analyses of released synchronous TM6 mouse mammary hyperplastic epithelial cells at 0 h (*0 h-control*) and the cells untreated (*control*) or treated with 5 μM MSA for 3 h after the cells were starved (STV) for 48 h and released by feeding with regular medium containing growth factors and serum for 6 h as described in "Materials and Methods." These data are representative of three independent determinations. *A*, images of 23 genes involved in cell cycle regulation pathway, two host genes (*β-actin* and *GAPDH*) as internal positive controls, and pUC18 from bacterial plasmid as a negative control. A coding grid for the filter also is presented. In *B*, the absorbance data for each set of analyses are shown. Values are mean ± SE. A summary of multivariate statistical analyses is also presented.

Statistical Summary of the Effects of MSA on gene expression using c-DNA array analysis

Regulatory molecules	Overall multivariate statistic for an effect due to treatment with MSA	Univariate analysis: significant components, direction of change MSA vs control
Cyclins	p=0.013	D3, increased, p=0.01
CDKs	p=0.031	None
INK family	p=0.018	p19, increased, p=0.01
Cip/Kip family	p=0.004	p21, increased, p=0.01 p27, increased, p=0.04
Rb/E2F	p=0.004	E2F, decreased, p=0.04

during the multivariate analysis, the evidence indicated probable effects of MSA on the D family of cyclins, members of both families of CKIs, and on expression of E2F.

Cyclin D_1 and Associated Molecules. Using synchronously growing TM6 cells, the effects of MSA on the levels of cyclin D1 and CDK4, and the binding of CDK4 to cyclin D1, cyclin D1-associated kinase activity and levels of P16 and P19 were investigated using a combination of immunoprecipitation, Western blotting, and/or kinase activity assays. The results are shown in Fig. 3*A*. For the reasons stated in the "Materials and Methods" section, all data were subjected to multivariate ANOVA. The results of this analysis, which are summarized in Fig. 3*A*, indicated highly significant effects of both MSA and duration of exposure (time; $P < 0.001$) on the proteins and/or activities reflected in Western blots also shown in Fig. 3*A*. This justified further statistical analyses of the data shown in Fig. 3*B* to identify the factors that accounted for these effects. As quantified in

A

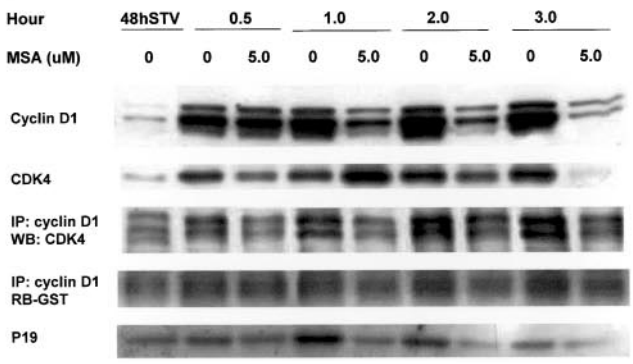

Mulitvariate Analysis: Overall test statistics (p-values)		Univariate F test for each factor included in the multivariate analysis (p-values)			
Factor	Overall	Factor	MSA	Time	MSA*Time
MSA	<0.01	Cyclin D1	0.001	0.737	0.131
Time	<0.01	CDK4	0.296	0.065	0.005
MSA*Time	<0.01	IP:D1-CDK4	0.009	0.077	0.521
		IP:D1-RBGST	0.000	0.000	0.001
		p19	0.000	0.000	0.000

B

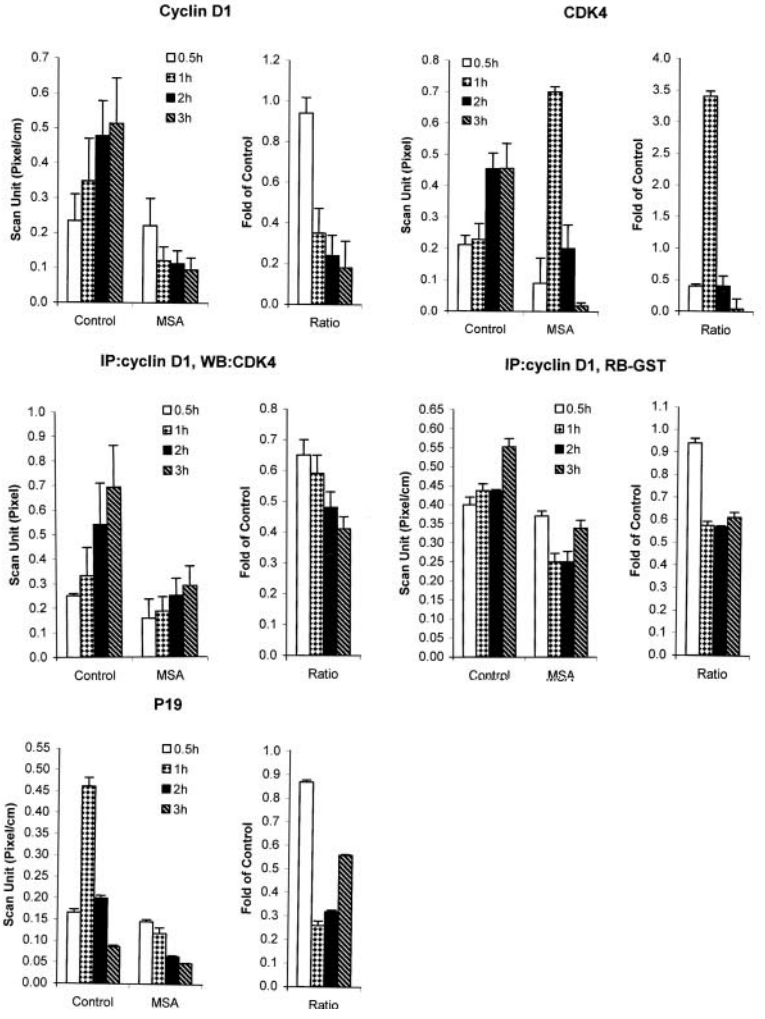

Fig. 3. Western blot analyses of cyclin D1, CDK4, cyclin D1-immunoprecipitated CDK4 (*IP:cyclin D1* and *WB:CDK4*), cyclin D1-associated kinase activity (*IP:cyclin D1* and *Rb-GST*), and P19 in synchronously growing TM6 cells. The cells were either untreated (control, 0 μM) or treated with 5 μM MSA for 0.5, 1, 2, and 3 h after the cells were starved (*STV*) for 48 h and released by feeding with regular medium containing growth factors and serum for 6 h as described in "Materials and Methods." These data are representative of three independent experiments. *A*, images of cyclin D1, CDK4, cyclin D1-immunoprecipitated CDK4, cyclin D1-associated kinase activity, and P19. A summary of the results of the simultaneous analysis of data for all of the molecules and from all three experiments using multivariate ANOVA also is presented. In *B*, the absorbance data for each set of analyses are shown. Values are mean ± SE.

Fig. 3*B*, levels of cyclin D1 protein in untreated cells tended to increase over time ($P = 0.066$), whereas in MSA-treated cells, cyclin D1 levels decreased, although the reduction was not statistically significant ($P = 0.138$). When levels of cyclin D1 protein in MSA-treated cells were expressed relative to levels observed in the untreated control cultures, relative levels were progressively lower over time ($P = 0.001$). The levels of CDK4 protein increased modestly in untreated cells over time ($P = 0.088$), whereas levels were variable and without a consistent pattern of change over time in MSA-treated cells ($P = 0.222$). The amount of CDK4 binding to cyclin D1 increased with time in the untreated cells ($P = 0.022$) but remained relatively constant over time in the MSA-treated cells ($P = 0.110$ for a linear increase over time). Consequently, relative to the amounts of the complex observed in untreated cells, the amount of cyclin D1-bound CDK4 in treated cells was 35, 41, 52, and 59% lower in MSA-treated cells at 0.5, 1, 2, and 3 h of the treatment ($P = 0.009$). The kinase activity in the pellet immunoprecipitated with cyclin D1 antibody increased over time in untreated cells ($P < 0.001$) but remained relatively constant in MSA-treated cells ($P = 0.849$). Kinase activity in MSA-treated cells was 94, 58, 57, and 61% of untreated control activity at 0.5, 1, 2, and 3 h ($P < 0.001$). Levels of P16 protein were investigated; however, this protein could not be detected under the experimental conditions used. Levels of P19 protein decreased over time in untreated ($P = 0.085$) and MSA-treated cells ($P < 0.001$). Overall, P19 levels were lower in MSA-treated cells than in untreated cells ($P < 0.001$).

Cyclin E and Associated Molecules. The effects of MSA on cyclin E and its associated regulatory molecules were also investigated in synchronously growing TM6 cells. All data were evaluated simultaneously using multivariate ANOVA. This analysis provided an estimate of both the overall statistical significance of the effects of MSA and time on this regulatory pathway, as well as on the individual components of the pathway. Whereas there is statistical evidence that activity of this cascade of events changed with MSA and time, none of the changes in any specific regulatory elements of the pathway were either of sufficient magnitude or of sufficient uniformity over time for differences attributable to MSA or time to be shown to be statistically significant by univariate ANOVA (data not shown). Similarly, differences in levels of P21, P27, and of the amount of these proteins complexed to cyclin E were variable and not influenced by treatment (data not shown).

Rb/E2F-1. The effects of MSA and of duration of treatment (time) on levels of hypo- and hyper-phosphorylated Rb and E2F-1 and on the binding of E2F-1 to Rb in synchronously growing TM6 cells are shown in Fig. 4. Levels of hypo-phosphorylated Rb were consistently higher, and the levels of hyper-phosphorylated Rb were lower in MSA-treated *versus* untreated control cells at all time points. Consequently, the ratio of hypo- to hyper-phosphorylated Rb was consistently higher in MSA-treated cells. Consistent with this pattern of response, levels of E2F-1 were lower in MSA-treated cells, and the magnitude of E2F-1 binding to Rb was elevated in these cells. In both the multivariate and the univariate ANOVAs, the effects of MSA and time on these molecules were highly significant statistically ($P < 0.001$).

Upstream Regulatory Pathways

As an initial inquiry, the effects of MSA were studied on two elements of a signal transduction pathway that could down-regulate cyclin D-mediated initiation of Rb phosphorylation, namely levels of IGF-IR and activation (phosphorylation) of Akt. As shown in Fig. 5, treatment of synchronized TM6 cells with MSA resulted in a significant suppression of levels of IGF-IR ($P < 0.01$). Levels of total Akt were not significantly altered by treatment with MSA; however, a significant suppression of levels of ppAkt was observed at each time point in MSA-treated cells relative to levels observed in untreated cells.

DISCUSSION

Until recently, the investigation of the cellular and molecular effects of selenium as a chemopreventive agent has been hampered by the lack of a compound that delivers and rapidly releases to the cell a form of selenium, methylselenol, which has been reported to be a proximal chemopreventive metabolite of the element. A recently introduced compound, MSA, overcomes this limitation and was used in the experiments reported in this study to probe in depth the origins of selenium's effects on cell cycle progression (7). The results discussed below are novel and potentially important in identifying a specific stage of the cell cycle that MSA modulates, the phosphorylation of Rb by cyclin D1-dependent kinase. In addition, evidence is reported that indicates that cyclin D1 kinase activity may be reduced because of the down-regulation of the IGF-I signaling pathway through the IP-3/Akt kinase cascade of events that promote cyclin D1-mediated phosphorylation of Rb.

After demonstrating that synchronized TM6 cells responded to MSA by inhibiting cell proliferation (Table 1) and arresting cells in the G_1 phase of the cell cycle (Fig. 1), we proceeded to perform an overall survey of the effects of MSA on a relatively comprehensive compilation of genes involved in cell cycle transit. A commercially available cDNA filter expression array was used for this purpose. Multivariate ANOVA was used to guide the interpretation of the data in an effort to identify patterns of gene expression likely to be affected by MSA. Those analyses, which are shown in Fig. 2, were interpreted to indicate that molecular events involved in the G_1-S transition were the most likely candidate target molecules through which MSA was exerting its effect.

Using immunoprecipitation in combination with Western blotting, the effects of MSA on cyclin D1 and cyclin E and their associated regulatory molecules were further investigated. As shown in Fig. 3, there was clear and consistent evidence that MSA suppressed cellular levels of cyclin D1 with parallel decreases in the amount of CDK4 immunoprecipitated with cyclin D1 and of the kinase activity associated with this complex. These data are interpreted to reflect a primary effect of MSA on cellular levels of cyclin D1. Efforts to detect P16 in the TM6 cell line were unsuccessful. However, it was possible to detect P19 protein. Whereas the gene array data indicated an increase in p19 message levels in response to MSA, the Western blot analysis detected less of this protein in MSA-treated cells. Although difficult to interpret without additional experiments, we speculate that these results reflect complex homeostatic cellular adjustments in the INK family of CKIs in response to the arrest of the cell cycle induced by MSA. The multivariate ANOVA indicated that cyclin E and its components were affected by MSA, a finding that would be anticipated based on the effects of MSA on cyclin D1 and its associated regulatory molecule; however, the magnitude of the effects were modest. When the results of the univariate ANOVAs were considered, none of the effects of MSA on individual components of the cyclin E pathway were found to be statistically significant. Thus, we hypothesize that the effects of MSA on this component of cell cycle regulatory machinery are secondary to the primary effects of MSA on cyclin D1-mediated phosphorylation of Rb. These findings are considered particularly important because cyclin D1 has been recognized as one of the oncogenes typically misregulated in breast cancer (23–25). Overexpression of cyclin D1 in the early G_1 phase of cell cycle and cyclin D1-associated activation occurs with high frequency

A

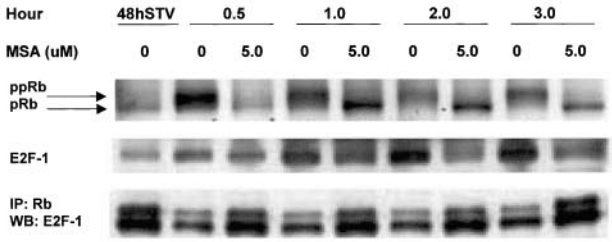

Mulitvariate Analysis: Overall test statistics		Univariate F-test for each factor included in the multivariate analysis			
Factor	Overall	Factor	MSA	Time	MSA*Time
MSA	<0.001	pRb	0.000	0.000	0.000
Time	<0.001	ppRb	0.000	0.000	0.000
MSA*Time	<0.001	pRb/ppRb	0.000	0.000	0.000
		E2F-1	0.000	0.000	0.000
		IP:Rb-E2F-1	0.000	0.000	0.000

B

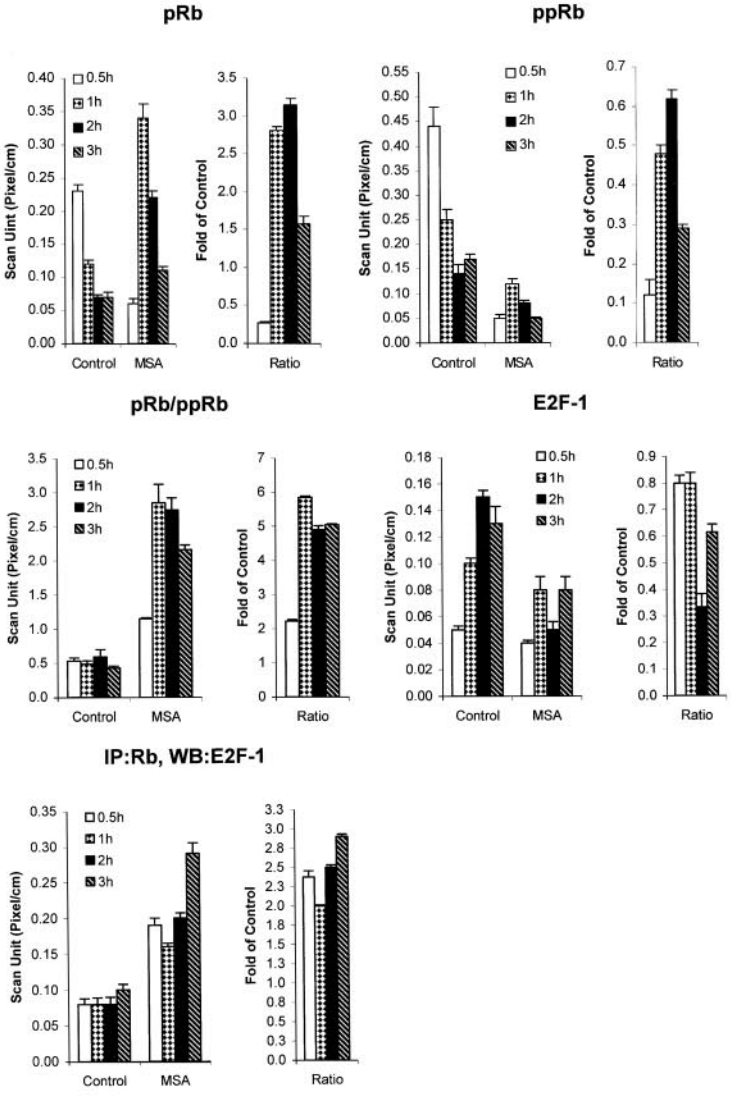

Fig. 4. Western blot analyses of Rb and E2F-1 Rb-immunoprecipitated E2F-1 (*IP:Rb* and *WB:E2F-1*) in synchronous TM6 mouse mammary hyperplastic epithelial cells (*STV*) and the cells untreated (control, 0 μM) or treated with 5 μM MSA for 0.5, 1, 2, and 3 h after the cells were starved (*STV*) for 48 h and released by feeding with regular medium containing growth factors and serum for 6 h as described in "Materials and Methods." These data are representative of results from three independent experiments. *A*, images of Rb (*ppRb*, hyper-phosphorylated Rb and *pRb*, hypo-phosphorylated Rb), E2F-1, and Rb-immunoprecipitated E2F-1. A summary of the results of the simultaneous analysis of data for all of the molecules and from all three experiments using multivariate ANOVA also is presented. In *B*, the absorbance data for each set of analyses are shown. Values are mean ± SE.

A

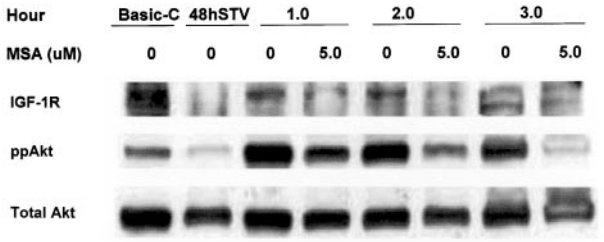

Mulitvariate Analysis: Overall test statistics		Univariate F-test for each factor included in the multivariate analysis			
Factor	Overall	Factor	MSA	Time	MSA*Time
MSA	<0.001	IGF-1R	0.011	0.302	0.884
Time	<0.001	ppAkt	0.007	0.175	0.720
MSA*Time	0.106	Total Akt	0.460	0.842	0.995

B

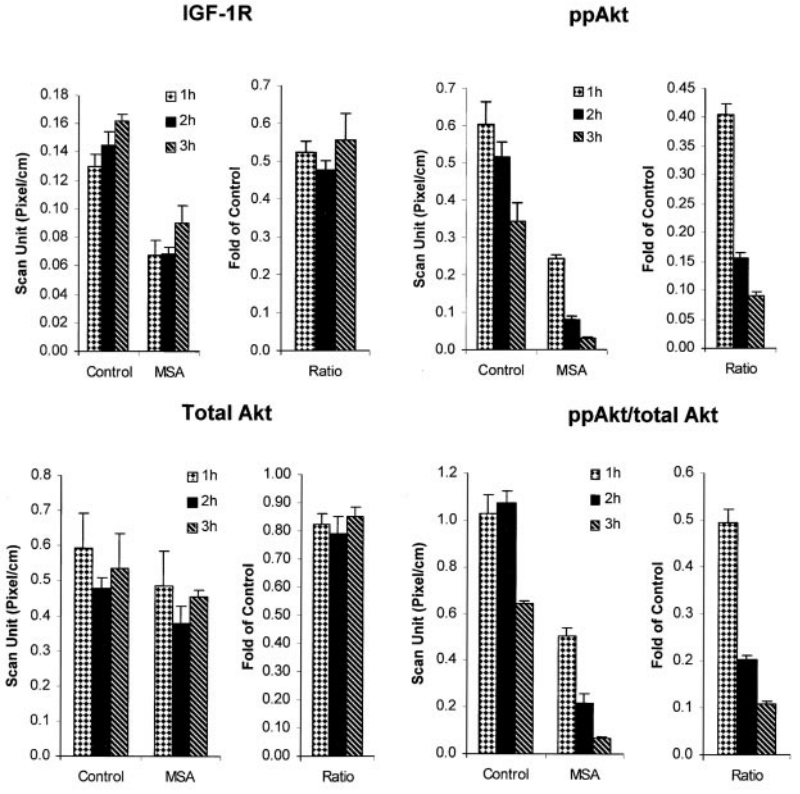

Fig. 5. Western blot analyses of IGF-IR, ppAkt, and total Akt in basic control TM6 mouse mammary hyperplastic epithelial cells (*Basic-C*, before starvation), synchronous TM6 mouse mammary hyperplastic epithelial cells (*STV*), and the cells untreated (control, 0 μM) or treated with 5 μM MSA for 1, 2, and 3 h after the cells were starved (*STV*) for 48 h and released by feeding with regular medium containing growth factors and serum for 6 h as described in "Materials and Methods." These data are representative of results from three independent experiments. *A*, images of IGF-IR, ppAkt, and total Akt. A summary of the results of the simultaneous analysis of data for all of the molecules and from all three experiments using multivariate ANOVA also is presented. In *B*, the absorbance data for each set of analyses are shown. Values are mean ± SE.

in human breast cancer and experimental mammary carcinogenesis (26–29). It has been demonstrated that overexpression of cyclin D1 results in abnormal mammary cell proliferation, including the development of mammary hyperplasias and adenocarcinomas (29, 30). Our findings that MSA down-regulated the level of cyclin D1 with inhibition of cyclin D1-associated cell cycle pathway are consistent with reports that MSA inhibits experimentally induced mammary cancer. It is noteworthy that other selenium compounds that can also increase intracellular pools of methylated forms of selenium also affect cyclin D1-Rb-associated phosphorylation and result in cell cycle arrest (10, 11, 31). This suggests that the effects of MSA may be generalizable to other chemopreventive forms of selenium.

The effect of MSA on cyclin D-CDK4 kinase activity shown in Fig. 4 led to the prediction that levels of hyperphosphorylated Rb would be low, and the binding of E2F-1 to Rb protein would be elevated in MSA-treated cells. The data shown in Fig. 4 are in agreement with this prediction. In evaluating these data, it is particularly notable that evidence of a shift between the hypophosphorylated and the hyperphosphorylated forms of Rb was found in untreated control *versus* MSA-treated cells. The effects of MSA on the phosphorylation of Rb were considerable in magnitude and were consistent over time. These data are consistent with the dramatic inhibition of cell cycle progression by MSA, as shown in Fig. 1.

In a final series of experiments, which was considered hypothesis generating, it was speculated that the effects of MSA could be mediated by down-regulation of the IGF signal transduction pathway. This idea was based on a number of publications that indicate that selenium can modulate IGF-I metabolism *in vivo* (32). As shown in

Fig. 5, a reduction in levels of IGF-IR-α was observed in response to MSA. It was predicted that down-regulation of this pathway would reduce phosphylated levels of Akt, and evidence in support of this hypothesis was also obtained. Hence, we propose that MSA blocks cell cycle progression in the early G_1 phase of the cycle primarily by limiting the availability of cyclin D1 for complexation with CDK4. We further propose that this effect is likely attributable to the accelerated degradation of cyclin D1, which has been reported to be a consequence of inhibiting the activation of Akt (33). It appears that the activation of Akt can be regulated by modulation of IGF-I signal transduction via a reduction in levels of the IGF-IR-α subunit of the receptor, which has been reported to play an active role in IGF-I mitogenic signaling (34). This hypothesis requires vigorous examination. Of particular interest in future studies would be the identification of the mechanism(s) that accounts for the apparent effect of MSA on IGF-IR-mediated mitogenic signaling.

REFERENCES

1. Ganther, H. E. Selenium metabolism, selenoproteins and mechanisms of cancer prevention: complexities with thioredoxin reductase. Carcinogenesis (Lond.), *20:* 1657–1666, 1999.
2. Ip, C. Selenium inhibition of chemical carcinogenesis. Fed. Proc., *44:* 2573–2578, 1985.
3. Medina, D., and Morrison, D. G. Current ideas on selenium as a chemopreventive agent. Pathol. Immunopathol. Res., *7:* 187–199, 1988.
4. Ip, C. Lessons from basic research in selenium and cancer prevention. J. Nutr., *128:* 1845–1854, 1998.
5. Clark, L. C., Combs, G. F., Jr., Turnbull, B. W., Slate, E. H., Chalker, D. K., Chow, J., Davis, L. S., Glover, R. A., Graham, G. F., Gross, E. G., Krongrad, A., Lesher, J. L., Jr., Park, H. K., Sanders, B. B., Jr., Smith, C. L., and Taylor, J. R. Effects of selenium supplementation for cancer prevention in patients with carcinoma of the skin. A randomized controlled trial. Nutritional Prevention of Cancer Study Group. JAMA, *276:* 1957–1963, 1996.
6. Ip, C., Zhu, Z., Thompson, H. J., Lisk, D., and Ganther, H. E. Chemoprevention of mammary cancer with Se-allylselenocysteine and other selenoamino acids in the rat. Anticancer Res., *19:* 2875–2880, 1999.
7. Ip, C., Thompson, H. J., Zhu, Z., and Ganther, H. E. *In vitro* and *in vivo* studies of methylseleninic acid: evidence that a monomethylated selenium metabolite is critical for cancer chemoprevention. Cancer Res., *60:* 2882–2886, 2000.
8. Dong, Y., Lisk, D., Block, E., and Ip, C. Characterization of the biological activity of γ-glutamyl-Se-methylselenocysteine: a novel, naturally occurring anticancer agent from garlic. Cancer Res., *61:* 2923–2928, 2001.
9. Sinha, R., Said, T. K., and Medina, D. Organic and inorganic selenium compounds inhibit mouse mammary cell growth *in vitro* by different cellular pathways. Cancer Lett., *107:* 277–284, 1996.
10. Zhu, Z., Jiang, W., Ganther, H. E., Ip, C., and Thompson, H. J. Activity of Se-allylselenocysteine in the presence of methionine γ-lyase on cell growth. DNA integrity, apoptosis, and cell-cycle regulatory molecules. Mol. Carcinog., *29:* 191–197, 2000.
11. Jiang, W., Zhu, Z., Ganther, H. E., Ip, C., and Thompson, H. J. Molecular mechanisms associated with Se-allylselenocysteine regulation of cell proliferation and apoptosis. Cancer Lett., *162:* 167–173, 2001.
12. Sinha, R., and Medina, D. Inhibition of cdk2 kinase activity by methylselenocysteine in synchronized mouse mammary epithelial tumor cells. Carcinogenesis (Lond.), *18:* 1541–1547, 1997.
13. Sinha, R., Kiley, S. C., Lu, J. X., Thompson, H. J., Moraes, R., Jaken, S., and Medina, D. Effects of methylselenocysteine on PKC activity, cdk2 phosphorylation and gadd gene expression in synchronized mouse mammary epithelial tumor cells. Cancer Lett., *146:* 135–145, 1999.
14. DelSal, G., Loda, M., and Pagano, M. Cell cycle and cancer: critical events at the G1 restriction point. Crit. Rev. Oncog., *7:* 127–142, 1996.
15. Sherr, C. J. Cancer cell cycles. Science (Wash. DC), *274:* 1672–1677, 1996.
16. Block, E., Birringer, M., Jiang, W., Nakahodo, T., Thompson, H. J., Toscano, P. J., Uzar, H., Zhang, X., and Zhu, Z. Allium chemistry: synthesis, natural occurrence, biological activity, and chemistry of Se-alk(en)ylselenocysteines and their γ-glutamyl derivatives and oxidation products. J. Agric. Food Chem., *49:* 458–470, 2001.
17. Zhu, Z., Jiang, W., Ganther, H. E., Ip, C., and Thompson, H. J. *In vitro* effects of Se-allylselenocysteine and Se-propylselenocysteine on cell growth. DNA integrity and apoptosis. Biochem. Pharmacol., *60:* 1467–1473, 2000.
18. Medina, D., Stephens, L. C., Bonilla, P. J., Hollmann, C. A., Schwahn, D., Kuperwasser, C., Jerry, D. J., Butel, J. S., and Meyn, R. E. Radiation-induced tumorigenesis in preneoplastic mouse mammary glands *in vivo*: significance of p53 status and apoptosis. Mol. Carcinog., *22:* 199–207, 1998.
19. Medina, D., Kittrell, F. S., Liu, Y. J., and Schwartz, M. Morphological and functional properties of TM preneoplastic mammary outgrowths. Cancer Res., *53:* 663–667, 1993.
20. Krishan, A. Rapid flow cytofluorometric analysis of mammalian cell cycle by propidium iodide staining. J. Cell Biol., *66:* 188–193, 1975.
21. Wu, X., Rubin, M., Fan, Z., DeBlasio, T., Soos, T., Koff, A., and Mendelsohn, J. Involvement of p27KIP1 in G1 arrest mediated by an anti-epidermal growth factor receptor monoclonal antibody. Oncogene, *12:* 1397–1403, 1996.
22. Snedecor, G. W., and Cochran, W. G. (eds.). Statistical Methods, Ed. 6. Ames, IA: Iowa State University Press, 1967.
23. Motokura, T., Bloom, T., Kim, H. G., Juppner, H., Ruderman, J. V., Kronenberg, H. M., and Arnold, A. A novel cyclin encoded by a bcl1-linked candidate oncogene. Nature (Lond.), *350:* 512–515, 1991.
24. Rosenberg, C. L., Kim, H. G., Shows, T. B., Kronenberg, H. M., and Arnold, A. Rearrangement and overexpression of D11S287E, a candidate oncogene on chromosome 11q13 in benign parathyroid tumors. Oncogene, *6:* 449–453, 1991.
25. Lammie, G. A., Fantl, V., Smith, R., Schuuring, E., Brookes, S., Michalides, R., Dickson, C., Arnold, A., and Peters, G. D11S287, a putative oncogene on chromosome 11q13, is amplified and expressed in squamous cell and mammary carcinomas and linked to BCL-1. Oncogene, *6:* 439–444, 1991.
26. Matsushime, H., Roussel, M. F., Ashmun, R. A., and Sherr, C. J. Colony-stimulating factor 1 regulates novel cyclins during the G1 phase of the cell cycle. Cell, *65:* 701–713, 1991.
27. Oyama, T., Kashiwabara, K., Yoshimoto, K., Arnold, A., and Koerner, F. Frequent overexpression of the cyclin D1 oncogene in invasive lobular carcinoma of the breast. Cancer Res., *58:* 2876–2880, 1998.
28. Gillett, C., Fantl, V., Smith, R., Fisher, C., Bartek, J., Dickson, C., Barnes, D., and Peters, G. Amplification and overexpression of cyclin D1 in breast cancer detected by immunohistochemical staining. Cancer Res., *54:* 1812–1817, 1994.
29. Zhu, Z., Jiang, W., and Thompson, H. J. Effect of energy restriction on the expression of cyclin D1 and p27 during premalignant and malignant stages of chemically induced mammary carcinogenesis. Mol. Carcinog., *24:* 241–245, 1999.
30. Wang, T. C., Cardiff, R. D., Zukerberg, L., Lees, E., Arnold, A., and Schmidt, E. V. Mammary hyperplasia and carcinoma in MMTV-cyclin D1 transgenic mice. Nature (Lond.), *369:* 669–671, 1994.
31. Ip, C., Thompson, H. J., and Ganther, H. E. Selenium modulation of cell proliferation and cell cycle biomarkers in normal and premalignant cells of the rat mammary gland. Cancer Epidemiol. Biomarkers Prev., *9:* 49–54, 2000.
32. Gronbaek, H., Frystyk, J., Orskov, H., and Flyvbjerg, A. Effect of sodium selenite on growth, insulin-like growth factor-binding proteins and insulin-like growth factor-I in rats. J. Endocrinol., *145:* 105–112, 1995.
33. Ramljak, D., Calvert, R. J., Wiesenfeld, P. W., Diwan, B. A., Catipovic, B., Marasas, W. F., Victor, T. C., Anderson, L. M., and Gelderblom, W. C. A potential mechanism for fumonisin B(1)-mediated hepatocarcinogenesis: cyclin D1 stabilization associated with activation of Akt and inhibition of GSK-3β activity. Carcinogenesis (Lond.), *21:* 1537–1546, 2000.
34. Dudek, H., Datta, S. R., Franke, T. F., Birnbaum, M. J., Yao, R., Cooper, G. M., Segal, R. A., Kaplan, D. R., and Greenberg, M. E. Regulation of neuronal survival by the serine-threonine protein kinase Akt. Science (Wash. DC), *275:* 661–665, 1997.

Mechanisms of Cell Cycle Arrest by Methylseleninic Acid

Zongjian Zhu, Weiqin Jiang, Howard E. Ganther, et al.

Cancer Res 2002;62:156-164.